An Antenna-filter codesign for cardiac implants

Emeric de Foucauld, Jean-Baptiste David, Christophe Delaveaud and Pascal Ciais
CEA-LETI
Grenoble, France
emeric.defoucauld@cea.fr

***Abstract*—This paper presents the design of a 2.4 GHz antenna and a BAW filter for cardiac implants in the ISM band. These components are both sensitive to their environment. The antenna modelisation in human body is presented in order to characterize its impedance. The BAW filter connection to a substrate modifies its impedance, so the link between the two components is the key of the Radio-Frequency transmission. The antenna-filter exhibits a Standing Wave Ratio better than 2 and a maximum insertion loss of 5.6 dB in the 2.4-2.48 GHz frequency band.**

Keywords: Filter, antenna, modelisation, cardiac implants, co-design

I. INTRODUCTION

In medical applications, there is a need for wireless communications between implanted devices (pacemaker, defibrillator) in human body and external instruments [1]. Recently, antennas for implanted devices have been successfully designed [2-6]. The 2.4 GHz frequency band (ISM) allows high data rate communication and smaller size devices than MICS band, but the attenuation of waves is bigger. Each stage of the RF chain should be optimized because the link budget is tight. The mismatch of impedance at the filter transceiver and antenna-filter has to be minimized. We present in this paper the co-design of a loop antenna and a BAW filter for a 2.4 GHz implant cardiac communication. In the antenna section we will discuss the human body effect and its constraints on the antenna impedance variation, the modelisation of the antenna into the body will be presented. Then the BAW filter integration will be shown and the connection to the antenna with the matched impedance will be presented.

II. ANTENNA

A. Modelisation

Generally, antenna impedance is characterized in homogeneous lossy dispersive fluids which simulate the average human body electrical properties. As accurate impedance characterization requires to reproduce the electromagnetic field behavior in near antenna area (reactive area), only a reduced volume of these lossy materials is modeled. But, to accurately take into account the near field pacemaker antenna behavior, different human tissues close to the implant have to be considered and carefully modeled. This will be done by using heterogeneous models with limited dimensions as multi-layered structures or as existing accurate human model of electromagnetic simulation tool. Only impedance results of [2-3] are presented in these heterogeneous models but no accurate comparisons were made with the homogeneous ones. However, antenna impedance in human body must be carefully known in order to correctly match the antenna to the RF front-end circuitry and then to optimize the implanted device performances. Nevertheless, we must specify that these kinds of limited-volume models are only suitable to assess implant antenna impedance. The characterization of the far field radiated by the implanted antenna (shape of patterns, level of gain), obtained using far field integral equations, needs to use a model with realistic dimensions of dielectric lossy materials, that is to say dimensions of a real human bust. However, the bust geometry doesn't need to be accurately defined and generally, a homogeneous model of the human tissues with global dimensions and shape is classically used [7]. Thereby, a human bust with large dimensions allows to correctly take into account associated effect on the propagation of electromagnetic fields (absorption, diffraction, scattering).

The objective of this part is to study antenna pacemaker input impedance in homogeneous and heterogeneous models and finally, showing that one of this model is more suitable to give correct and precise impedance characteristics. The targeted impedance to connect the filter is 100 Ohms.

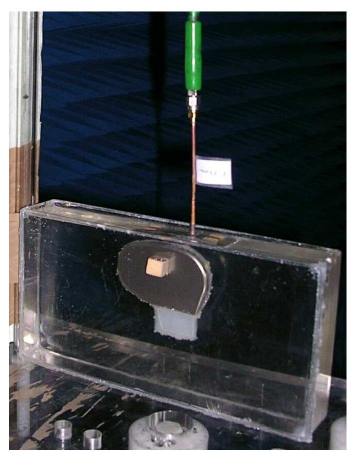

Figure 1. Experimental set up

978-3-9810801-7-9/DATE11/©2011 EDAA

B. Homogeneous problem

The medical implantable prototype device includes a housing case made of titanium ($\sigma = 2.3.10^6$ S/m) and a miniature magnetic loop antenna made of copper ($\sigma = 5.8.10^7$ S/m). The compact loop, covered by a non lossy header in silicone (ε_r = 2.8), is fed by a coaxial cable: the two extremities of the loop are respectively connected to the inner and the outer conductor of the RF feed cable. The outer conductor of the cable is grounded to a single-face PCB made of FR4 substrate (ε_r = 4.9 and tg δ = 0.025) positioned inside the housing case. No specific precautions have been taken in order to limit the influence of the RF feed cable [8], because some comparisons between measured and simulated results in free space with and without housing case allow to determine that the housing case acts as an efficient ground plane that isolates loop antenna from coaxial cable influence. Except for the metallic housing case in titanium, all other materials used are not biocompatible but were chosen in order to simplify the experimental realization of the whole prototype device. The communication between an exterior electronic device and the pacemaker loop antenna is typically done over an inductive link (near field systems) [9]. However, results shown in this paper are suitable for a propagating electromagnetic wave (far field propagation properties). The pacemaker implant is plunged in a dispersive and lossy liquid material with frequency dependent electrical properties. In order to characterize antenna pacemaker impedance in the 2400-2480 MHz band, the 2450 MHz body tissue equivalent liquid is used. The target electrical parameters of this fluid (conductivity σ and real part of permittivity ε_r') are provided by the FCC [10]. In the electromagnetic simulation tool based on Finite-Integration Time-Domain (FITD) method (CST Microwave Studio) [11], the homogeneous liquid model is represented by a parallelepiped (15 cm x 11 cm x 3.4 cm). The rectangular homogeneous block dimensions and the pacemaker location inside it, are optimized for the heterogeneous model For the experimental setup (Figure 1). The pacemaker is plunged into a rectangular plastic recipient filled with homogeneous liquid. This recipient has the same dimensions than the simulated one.

C. Heterogenous problem

The implantable device is inserted in three heterogeneous models: first, the heterogeneous human model named Hugo which is the simulation tool human model [12], then a multi-layered structure and lastly, a simple experimental setup made to validate simulated heterogeneous models, the "human + hand" model. Compared to previous homogeneous model, the main advantage of these heterogeneous models is to carefully model predominant layers of human tissues near antenna area and then, to accurately take into account the near field pacemaker antenna behavior.

1) Human model of simulation tool (Hugo)

The pacemaker device is implanted in the pectoral of Hugo, in a limited volume sample of 11.2 x 6.4 x 11.6 cm^3 to limit simulation time. The voxel size of the human body model is the minimal voxel size of the simulation tool, i.e. 1 mm^3. The whole body phantom contains 44 different tissues, whose real part of permittivity (ε_r') and conductivity (σ) are taken from [13] at 2450 MHz. Obviously, the chosen limited sample includes fewer tissues than the complete body model.

2) Multi-layered model

In order to easily design implanted antennas, multi-layered geometries which provide an acceptable model for the human body, were firstly proposed in [1]. Based on the real human body structure of the simulation tool, the heterogeneous multi-layered model used here is made of three layers (skin, fat, muscle) that have different thickness and different electrical properties. The thickness of the skin, fat and muscle tissues are respectively 4, 20 and 10 mm. The electrical properties of these three layers are taken from electrical data of human body phantom tissues. The pacemaker is implanted in the fat layer just under the skin layer. The geometrical characteristics of the heterogeneous model, i.e. pacemaker position inside the rectangular block and dimensions of both layers and whole block, have been optimized in order to be in accordance with Hugo implant impedance.

3) "Human + hand" model

In order to validate heterogeneous simulated models, a simple experimental setup with a real human is made. This one covers the pacemaker with his hand and puts it against his bust in exercising a strong pressure (Figure 2). This setup has not the intention to replace an implantation in a realistic human body, but we will see in the next section that it constitutes a good approximation.

D. Results

In homogeneous models, measured results with coaxial cable are systematically compared to simulated results with and without cable. In the configuration without cable, the loop antenna is fed by a lumped port which consists typically in a voltage applied between the two extremities of the loop. This configuration was used in order to simplify the numerical problem size to solve and thereby to reduce the total simulation time.

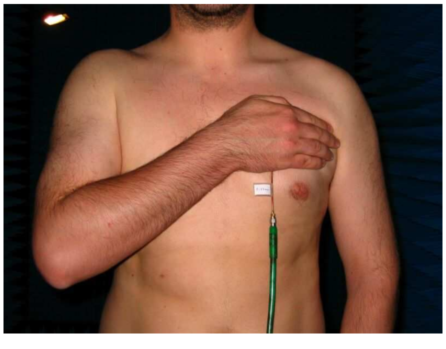

Figure 2. “Human+ hand” model

Finally, only this simplified excitation setup will be used in accurate and heavy heterogeneous models because it allows fast simulation results to be obtained.

Simulated antenna pacemaker input impedances in homogeneous model are in reasonable agreement with the measured one. Simulated results with and without cable are in very good accordance. So, these results allow the validation of the excitation without cable and the following use of lumped port in heterogeneous models. Moreover, the experimental characterization of antenna pacemaker impedance in homogeneous lossy fluid allows validation of optimized simulated models. In particular, impedance result of the special experimental setup is not far away from both simulated multi-layered and human model curves. We consider impedance result of Figure 3 is a good experimental approach that enables validation of simulated models. After studying impedance characteristics for each group of models separately, a global comparison is considered now. The main difference from results of homogeneous and heterogeneous models comes from the position of the resonant frequency. These impedance errors between homogeneous and heterogeneous models are too significant to be neglected.

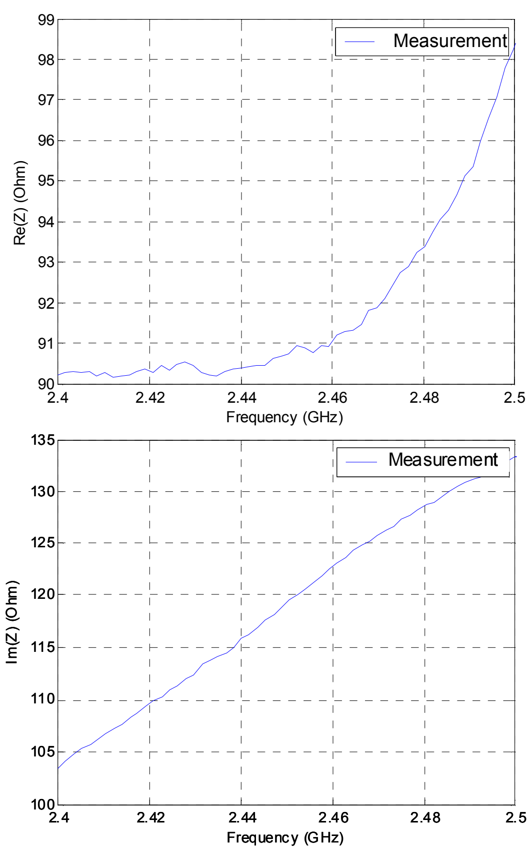

Figure 3. Impedance measurement of Human+hand model

To allow maximum power transfer between transceiver circuitry and antenna, RF front-end designers must exactly know antenna impedance values in the frequency band of interest. Consequently, correct antenna input impedance of implant device must be characterized in accurate heterogeneous models because, thanks to precise modelisation of all human tissues in near antenna area, this kind of model takes carefully into account the near field pacemaker antenna behavior. We have also determined that both exact location of the pacemaker device in the realistic human model and exact layer thickness of the multi-layered model have a non-negligible effect on the antenna input impedance. Accurate comparison between pacemaker antenna input impedance in homogeneous and in heterogeneous models was presented. The validation of simulated homogeneous and heterogeneous models by experimentation was obtained. The results reveal that to characterize correct antenna impedance, accurate heterogeneous models as multi-layered structures or as human model of electromagnetic simulation tool must be imperatively used. As all implanted patients have not the same corpulence and constitution, a perspective of this work should be to characterize the input impedance sensitivity of the heterogeneous models by varying implant position, layers thickness and layers electrical properties. It should be done to exactly know the variation range of input impedance in order to estimate antenna mismatching problems with RF front-end circuit.

III. BAW

This part deals with the BAW technology, BAW filter simulation methodology, and comparison between design and measurements for an ISM Band 2.44GHz SMR-BAW filter.

A. *Technology*

The filter was implemented using SMR type resonators (Solidly Mounted Resonators). The resonators in SMR structures are realized on top of an acoustic mirror structure based on the Bragg Reflector principle [14]. The acoustic mirror presents an optimum discontinuity for reflecting the acoustic waves at the interface with the bottom electrode, confining the waves into the main resonant structure. The realization of BAW filters is largely based on standard microelectronics process: thin film deposition, photo-lithography, dry or wet etch and stripping. The filter stack can be divided into resonators' layers (electrodes and piezoelectric layer), Bragg reflector's layers and micro-packaging (Fig. 4). The resonator layers were composed of the classical couple AlN-Mo. However, in contrast to [15] we have implemented the Bragg reflector using an exclusive dielectric stack composed of SiOC:H and SixNy. The acoustical performance (acoustic coupling around 6.5% and Q factors around 800) of the fully-dielectric stack is comparable to traditional SiO2-W reflectors. However, this fully-dielectric configuration strongly reduces the electrical coupling between resonators, and ensures high out-of-band rejection. Zero-level packaging ensures a micro-cavity on the upper side of the resonator, thanks to a released bi-layer SiO2/BCB.

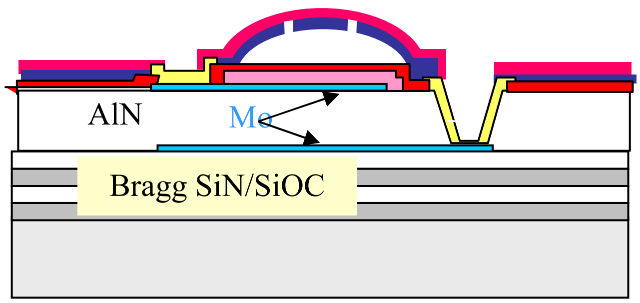

Figure 4. BAW-SMR stack (Bragg, Resonator and packaging).

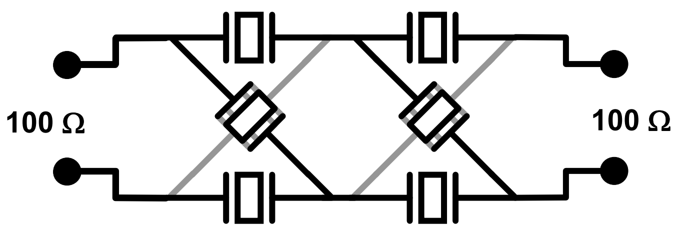

Figure 5. Double Lattice BAW filter topology.

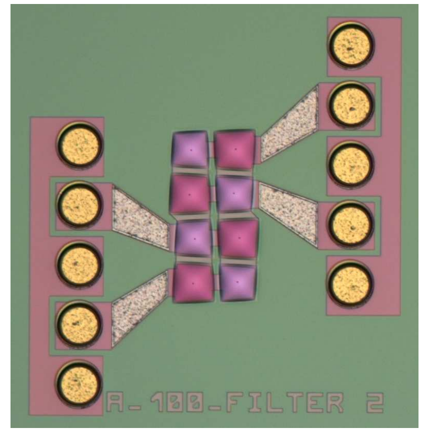

Figure 6. Double Lattice BAW filter photography.

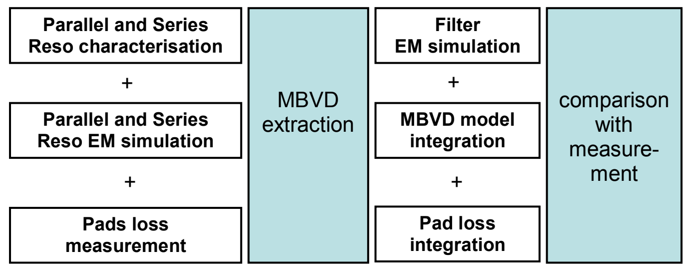

Figure 7. Design and backward analysis methodology.

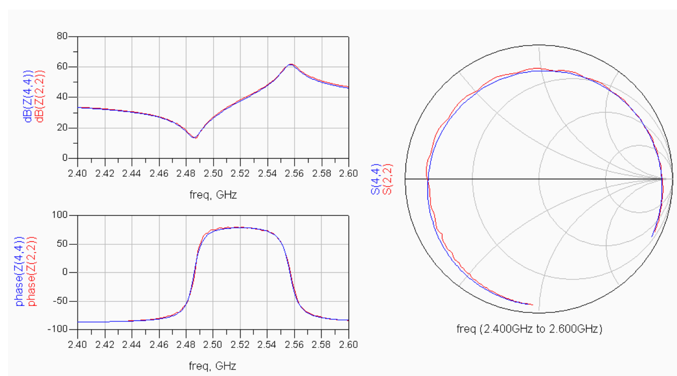

Figure 8. Fit between a MBVD model and a measured resonator.

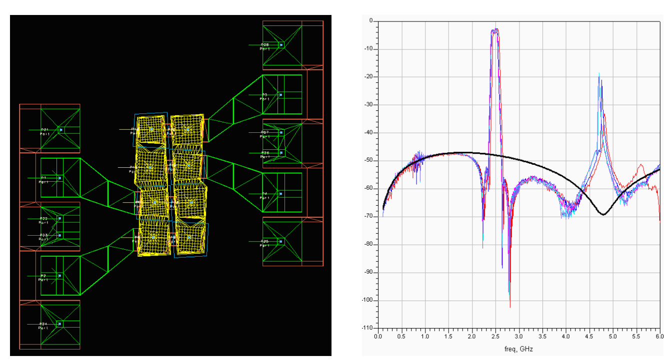

Figure 9. 2.5 D EM simulation and comparison with filter measurement.

B. Design

The filter is based on a double-lattice topology (Fig.5), and series inductances of maximum 1nH can be added so as to increase slightly the bandwidth, or for matching considerations. The photography Fig.6 shows one of the 2.4GHz filter. The active area is 450x225µm^2, and the complete die is 1mm^2. 120µm diameter areas with a 150µm pitch were prepared for bumping as well as for probe testing.

C. Simulation and results

The simulation methodology for BAW filter is based on prototype resonator characterization, Modified Butterworth-Van-Dyke models and electromagnetic tools. The synopsis, which is also used for backward analysis, is given Fig.7. According to this methodology, an operant intrinsic MBVD model fits with a dedicated technology stack, and does not depend on the design (Fig.8). This elementary brick is employed in electrical simulations, leading to a close-to-final layout, which is evaluated by planar EM simulation. This step gives a realistic response of this part of the filter (Fig.9) which is due to electromagnetic coupling, thus especially the out-of-band rejection. The acoustic effects must be implemented in this EM simulation (by including intrinsic MBVD model) to make filtering function appear. The complete electrical-acoustic-electromagnetic simulation of such a filter is shown in the figure 10. The filter exhibits almost 100MHz band at 3dB IL. But techno issues lead to 30MHz center frequency shift.

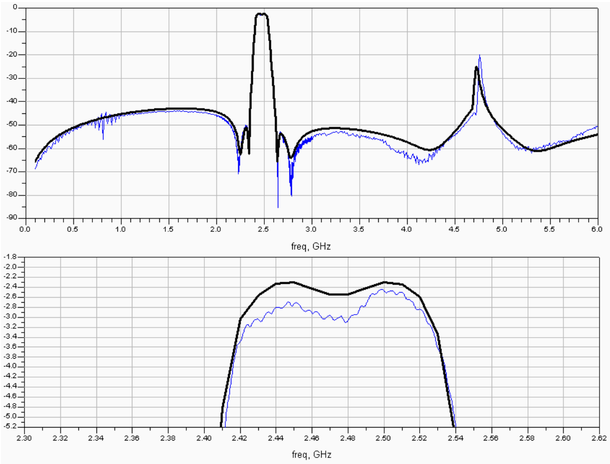

Figure 10. Complete simulation of a 2.44GHz BAW filter, and comparison to measurement

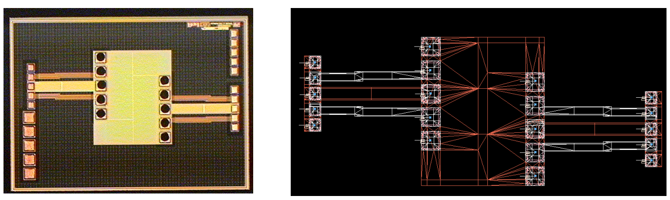

Figure 11. Pattern and EM mesh for BAW flip-chip on CMOS.

IV. Filter Integration and Co-Design

In this part, we first present the different ways to connect the BAW filter to a substrate: directly on the CMOS 2.4 GHz transceiver chip and on LTCC substrate. Then, the filter functionality associated to the antenna is given.

A. *Flip-chip on CMOS*

In a first approach of the matching-filtering integration, the BAW filter is supposed to be flip-chipped on the CMOS circuit which contains the 2.44GHz RF-frontend. The bump pitch and diameter is lead by flip-chip technology. Bumps are 120µm wide and must be located with a minimum distance of 150µm. In order to test this approach, the BAW filter is flip-chipped on a test pattern which is shown in Fig.11. The EM simulation of the pattern with the EM-acoustic simulation of the BAW filter allows to perform a global simulation that we compare with the measurement of the flip-chipped BAW. This comparison is shown in the next figure. This integration approach exhibits limited performances for several reasons. The CMOS technology is based on a lossy substrate which gives low performances interconnects. As consequences, wide pad bumps are strongly capacitive, and minimum distance between bumps and pad ring gives long and lossy lines. In the figure 12, we can see two effects: the filter mismatch (giving a deep ripple) and stronger insertion loss compared to the standalone filter.

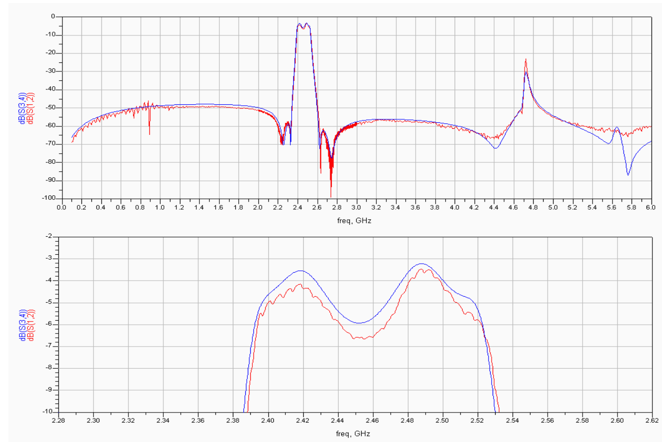

Figure 12. BAW flip-chip on CMOS, comparison with simulation.

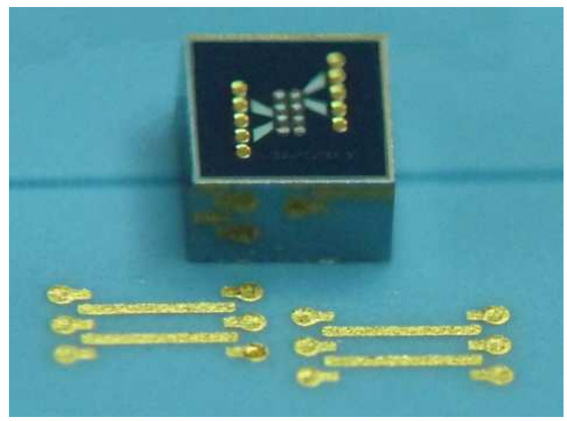

Figure 13. LTCC pattern with a BAW die ready for flip-chip.

B. *Flipchip on LTCC*

The flip-chip on CMOS was motivated by a strong integration; unfortunately, the electrical behavior didn't match with the product specifications. In order to get a better performance in the Antenna-to-CMOS link, an alternative design has been investigated to assemble BAW filter with the antenna matching network in a same LTCC die, leading to a SiP approach.

A test pattern on LTCC was done to directly compare the BAW performances with the flip-chip on CMOS (Fig.13). The LTCC was a 2-layer Dupont 951, with postfired Au on the upper surface, and Ag for internal layer. This one was used for ground plane.

The figure 14 shows the comparison between one on-probe BAW measurement, and the same flip-chipped BAW on LTCC. We can see that responses are very close each other. Less than 0.2dB additional insertion loss is observed.

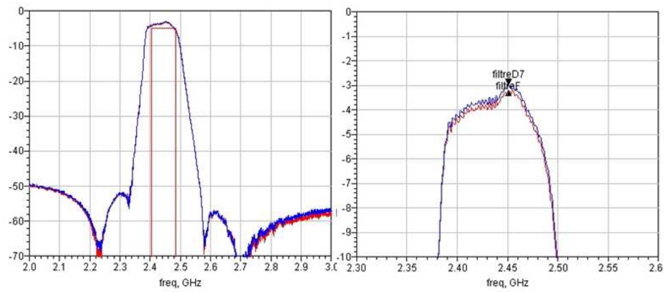

Figure 14. Comparison between stand alone and flip-chip on LTCC.

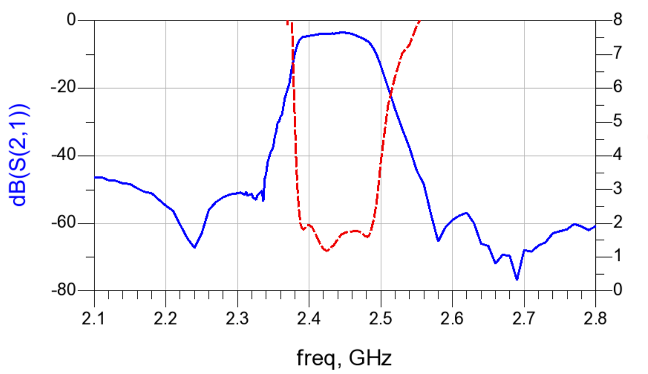

Figure 15. Antenna-to-RF Front-end path analysis

C. *Antenna-filter response.*

The filter response on LTCC being promising, we used this measurement and the database of Murata SMD components to investigate a complete Antenna-to-RF Front-end path, by a mix of electromagnetic simulation and measurement files. The path insertion loss is given in the S21 parameter of Fig.15, which exhibits a maximum IL of 5.6dB with the previous BAW filter. Thus, only 1dB IL is due to the complete integration strategy. The Standing Wave Ratio at the antenna port is better than 2 for a S11 at the BAW input better than 11dB.

V. Conclusion

This paper presents the modelisation of a RF link at 2.4 GHz between a BAW filter and an antenna. Simulations and measurement of an antenna into such environment was discussed. The antenna and the BAW filter impedances were matched and the Standing Wave Ratio is better than 2 with an insertion loss of maximum 5.6 dB. The next step of this work is the fabrication of the matching module and radiation measurements with the antenna.

Acknowledgment

This work was realized in the context of the EURIMUS project EPADIMD EM91 (European Platform for ADvanced active Implantable Devices). The authors would like to thank Sorin Group for providing liquids and pacemaker samples, Biotronik and MSE.

References

[1] R. Bashirullah, Wireless Implants ,Microwave Magazine, IEEE Volume: 11 , Issue: 7 , Part: Supplement Publication Year: 2010, Page(s): 14 - 23

[2] J. Kim and Y. Rahmat-samii, "Implanted antennas inside a human body : simulations, designs and characterizations", *IEEE Transactions on Microwave Theory and Techniques*, Vol. 52, No. 8, August 2004, pp. 1934-1943.

[3] P. Soontornpipit, C.M. Furse and Y.C. Chung, "Design of implantable Microstrip Antenna for communication with medical implants", *IEEE Transactions on Microwave Theory and Techniques*, Vol. 52, No. 8, August 2004, pp. 1944-1951.

[4] P. Soontornpipit, C.M. Furse and Y.C. Chung, "Miniaturized biocompatible microstrip antenna using genetic algorithm", *IEEE Transactions on Antennas and Propagation*, Vol.53, No.6, June 2005, pp. 1939-1945.

[5] C.-M. Lee, T.-C. Yo, C.-H. Luo, C.-H. Tu and Y.-Z. Juang, "Compact broadband stacked implantable antenna for biotelemetry with medical devices", *Electronic Letters*, Vol. 43, No. 12, June 2007, pp. 660-662.

[6] Wei Xia; Saito, K.; Takahashi, M.; Ito, K.; “Performances of an Implanted Cavity Slot Antenna Embedded in the Human Arm” Antennas and Propagation, IEEE Transactions on Volume: 57 , Issue: 4 , Part: 1, 2009 , Page(s): 894 - 899 .

[7] W.G. Scanlon, N.E. Evans and J.B. Burns, “FDTD analysis of a close-coupled 418 MHz radiating devices for human biotelemetry”, Phys. Med. Biol., Vol. 44, n°2, pp. 335-345, Feb. 1999.

[8] C. Icheln, J. Ollikainen and P. Vainikainen, ”Reducing the influence of feed cables on small antenna measurements”, Electronics Letters, Vol. 35, n°15, pp. 1212-1214, July 1999.

[9] A. Johansson, A. Karlsson, W. Scanlon, N. Evans and Y. Rahmat-samii, “Medical implant communication systems”, Antennas and propagation for body-centric wireless communications, P. S. HALL and Y. HAO, Artech House Inc., Chapter 6, pp 241-270, 2006.

[10] "Evaluating compliance with FCC guidelines for human exposure to radiofrequency electromagnetic fields", Office Eng, Technol., FCC, Washington DC, FCC OET Bull. 65, Supp. C.

[11] "Agilent 85070E dielectric probe kit 200 MHz to 50 GHz", Technical overview, Agilent literature number 5989-0222EN, October 25, 2006.

[12] CST Microwave Studio, Computer System Technology, GmbH, Darmstadt, Germany.

[13] http://www.fcc.gov/fcc-bin/dielec.sh

[14] K. M. Lakin, K. T. McCarron et R. E. Rose. "Solidly mounted resonators and filters". IEEE Utrasonics Symposium Proceedings, vol.: 2, pp.: 905-908. Seattle, 1995.

[15] R. Aigner et al. “Bulk-Acoustic-Wave Filters: Performance Optimization and Volume Manufacturing”. IEEE MTT-S 2003. pp. 2001-2004.